Photoemission Cross Sections for Fragments and Molecular Ions Produced by Collisions of He($2\,^3S$) Atoms with $SiCl_4$ and $GeCl_4$

Ikuo Tokue,* Hiroyuki Tanaka, and Katsuyoshi Yamasaki

Department of Chemistry, Faculty of Science, Niigata University, Ikarashi, Niigata 950-2181

(Received April 19, 1999)

Photoemissions from excited fragments and molecular ions produced by collisions of He($2\,^3S$) with $SiCl_4$ and $GeCl_4$ have been studied at the relative collision energy of 120—210 meV. Total emission cross sections in the 200—760 nm range for $SiCl_4$ and $GeCl_4$ are evaluated to be 4.5±0.8 and 2.2±0.4, respectively, in 10^{-20} m^2 units. Emission cross sections for $SiCl_4^+(\tilde{C}–\tilde{X})$, $GeCl_4^+(\tilde{C}–\tilde{X})$, and Ge I atomic lines slightly decrease with increases in the collision energy. This originates from the fact that the effective potentials of He($2\,^3S$) with $SiCl_4$ and $GeCl_4$ are slightly attractive. The branching ratio of Ge I states observed from $GeCl_4$ is consistent with a simple dissociation model assuming equipartition of the available energy. These results are compatible with the harpoon mechanism as an initial step for formation of Ge I from $GeCl_4$. The emission cross section for the SiCl(B′–X) band increases with the collision energy. This indicates that the effective potential between He($2\,^3S$) and $SiCl_4$ is repulsive, and that the SiCl(B′) state seems to be produced directly from $SiCl_4$ by an excitation transfer mechanism via superexcited states.

Formation of excited fragments resulting from the collisions of He* metastable atoms with Group 14 tetrachlorides has been studied by optical spectroscopy at thermal energy. Tsuji et al.[1—3] studied emissions from $SiCl_4$, $GeCl_4$, and $SnCl_4$ produced in the flowing helium afterglow from an interest in new spectroscopy of ionic species. They analyzed the new $SiCl^+(a–X)$, $GeCl^+(a–X)$, and $SnCl^+(a–X)$ transitions. Lambert et al.[4] have reported two broad emissions in the visible region produced by electron impact ionization, Penning ionization using He* and Ne* metastables, and photoionization of $SiCl_4$ and $GeCl_4$. These bands were assigned to the $\tilde{C}–\tilde{X}$ and $\tilde{C}–\tilde{A}$ bands of molecular ions. We have reported the emission cross sections of the Sn I atomic lines produced from the collision of He($2\,^3S$) with $SnCl_4$ and $Sn(CH_3)_4$;[5] the effective potential of He($2\,^3S$) with the target and formation mechanism of Sn I were discussed on the basis of the dependences of their emission cross sections on the collision energy. Nevertheless, there is only a little information about the dissociation mechanism of other Group 14 chlorides, especially at higher collision energies. The interaction of a target molecule with He($2\,^3S$) and its decay process are more complicated than that with a photon or an electron. Therefore, the knowledge of the interaction potential of the target molecule with He($2\,^3S$) is required for quantitative understanding of the dissociation dynamics.

This paper reports state-resolved emission cross sections (σ_{em}) for fragments and parent ions observed from $SiCl_4$ and $GeCl_4$ by using a crossed-beam method and the dependence of σ_{em}'s on the collision energy, and discusses the effective potentials with He($2\,^3S$) correlating to formation of the observed species and their reaction dynamics.

Experimental

The apparatus and experimental details for the fluorescence measurement have been reported previously.[5,6] In brief, He($2\,^3S$, $2\,^1S$) atoms are produced with a nozzle discharge source[7] and skimmed into a collision chamber; the singlet component of the total He* flux was estimated to be about 10%. Although no quench lamp was used to remove the He($2\,^1S$) component, its contribution to σ_{em} data was estimated to be within experimental errors. Under typical stable operating conditions, the discharge current was 10—30 mA, the voltage was 400—750 V, and the pressure of residual gas at the collision chamber measured by an ionization vacuum gauge was 2.7 mPa. The samples of $SiCl_4$ (stated purity of 99%) and $GeCl_4$ (stated purity of 99.99%) commercially obtained were used after degassing.

The fluorescence resulting from the collision of He($2\,^3S$) with target molecules was observed in a direction perpendicular to both the molecular and He* beams. The photons dispersed with a SPEX 1702 monochromator were monitored by combining a Hamamatsu R585 or R649S photomultiplier with single photon counting electronics. The relative sensitivity of the photon-detection system was calibrated with a deuterium lamp in the 200—310 nm region and with a halogen lamp by combining a cut-off filter (Toshiba UV-33 or Y-46) in the 310—760 nm region. In this study, σ_{em} for the fluorescence produced by collisions of He($2\,^3S$) was evaluated by comparing its emission intensity with that of the following Penning ionization:

$$He(2^3S) + N_2 \rightarrow N_2^+(B^2\Sigma_u^+) + He + e^-. \quad (1)$$

We have adopted the σ_{em} value of $(3.2\pm0.3)\times10^{-20}$ m^2 for reference reaction 1 at a relative collision energy (E_R) of 140 meV; this value was estimated from Fig. 5 in Ref. 8. The total emission intensity of the $N_2^+(B–X)$ system was derived from the observed intensities of the 0–0 and 1–0 bands by using the scaling factors calculated by Comes and Speier.[9]

Velocity distributions of the He* beam were observed by measuring the time of flight (TOF) from a chopper disk to a detector. The TOF spectrum of the He* beam observed under typical discharge conditions could be represented by a Maxwell–Boltzmann distribution. The root-mean-square velocity (v_M) thus derived almost coincides with the most probable velocity for each TOF spectrum. The average kinetic energy (E_M) of the He* beam derived from v_M was found to increase with the discharge power at the beam source.[5] In the fluorescence measurement, we could not use the chopped He* beam because of weak fluorescence intensity. Thus, we have controlled the kinetic energy of the He* beam by varying the discharge power. Therefore, it should be mentioned that σ_{em} values were measured with a relatively broad kinetic energy distribution; for instance the half width half maximum of the He* beam was 40 meV for E_M = 120 meV and 86 meV for E_M = 220 meV. The collision energy dependence of σ_{em} was obtained by converting the function of v_M into that of the relative collision energy (E_R) with the relation between E_R and the reduced mass (μ) of the He + target system,

$$E_R = \mu(v_M^2 + 3kT/m)/2, \quad (2)$$

where T is the temperature (300 K) and m is the mass of the target molecule.

Results and Discussion

Emission Spectra. Photoemissions produced by collision of He(2 ^{3}S) with $SiCl_4$ and $GeCl_4$ were observed at the relative collision energy (E_R) of 120—210 meV. Figure 1 shows a fluorescence spectrum in the 200—750 nm region produced from $SiCl_4$. Observed spectra have been assigned as the $B^2\Sigma^+$–$X^2\Pi$, $B'^2\Delta$–$X^2\Pi$, and $C^2\Sigma^+$–$X^2\Pi$ bands of SiCl and the $\tilde{C}^2T_2$–$\tilde{X}^2T_1$ and $\tilde{C}^2T_2$–$\tilde{A}^2T_2$ bands of $SiCl_4^+$, which correspond to reported spectral data.[4,10,11] We could identify neither the Si I line nor the SiCl ($A^2\Sigma^+$–$X^2\Pi$) band,[12] which were observed in the flowing helium afterglow.[1] This indicates that formation of excited Si atoms and SiCl(A) was negligible in this experiment.

Figures 2 and 3 show spectra produced from $GeCl_4$. Observed peaks in the 260—360 nm have been assigned as the Ge I resonance lines. In the assignment, we used transition

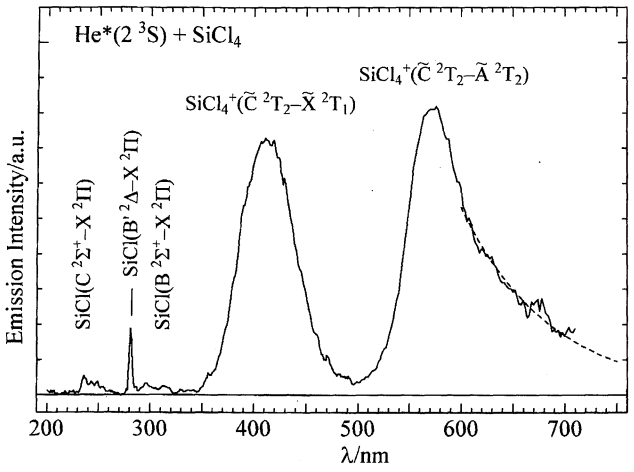

Fig. 1. Fluorescence spectrum resulting from collision of He(2 ^{3}S) with $SiCl_4$ at a relative collision energy of 150 meV with the optical resolution of 0.6 nm (fwhm); the optical sensitivity is calibrated.

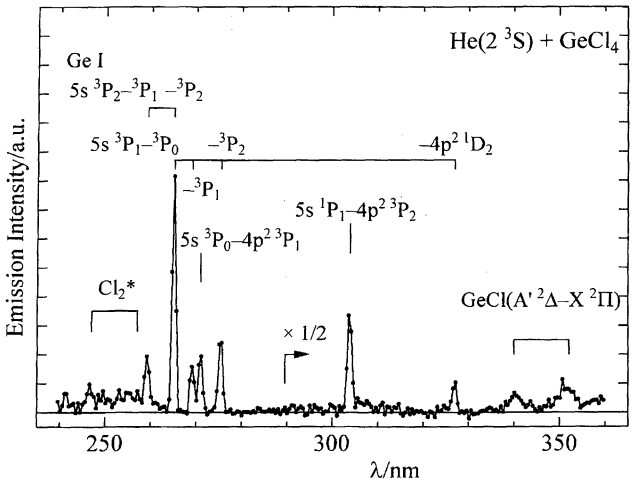

Fig. 2. Fluorescence spectrum in the 240—360 nm resulting from collision of He(2 ^{3}S) with $GeCl_4$ at a relative collision energy of 150 meV with the optical resolution of 0.6 nm (fwhm); the optical sensitivity is calibrated.

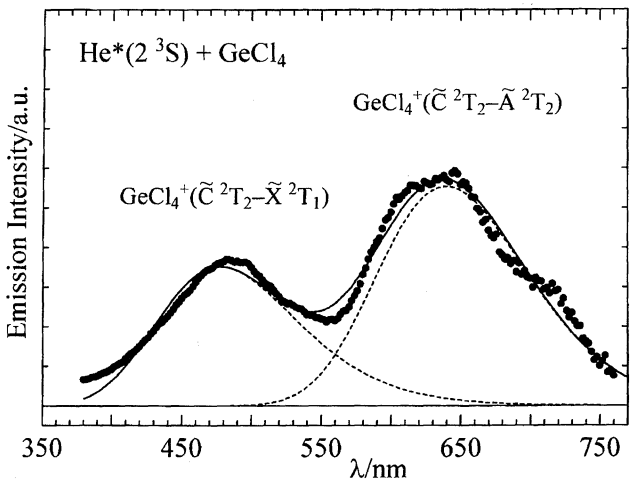

Fig. 3. Same as Fig. 2 in the 370—760 nm with the optical resolution of 1.2 nm: (•) for the observed spectrum, the solid and broken lines represent the synthetic spectrum and Gaussian function, respectively, fitted by a least-square method.

frequencies and wavelengths for Ge I or Ge II resonance lines calculated from the electronic energies of corresponding Ge I or Ge II states.[13] A weak GeCl ($A'^2\Delta$–$X^2\Pi$) band[14] at 340 and 352 nm and the Cl_2^* emission have also been observed, but neither the $A^2\Sigma^+$–$X^2\Pi$ band[15] nor the $B^2\Sigma^+$–$X^2\Pi$ band[16] of GeCl were identified. Two broad bands in the 380—760 nm have been attributed to the $\tilde{C}^2T_2$–$\tilde{X}^2T_1$ and $\tilde{C}^2T_2$–$\tilde{A}^2T_2$ systems of $GeCl_4^+$.[4] The shoulder around 720 nm may be caused by overlapping with the other band; although we do not know the spectroscopic data, the $GeCl_4^+$ ($\tilde{C}^2T_2$–$\tilde{B}^2E$) transition seems to be the most probable candidate since this band is expected to appear around 678 nm from the corresponding ionization potentials.[17] Nevertheless, we do not discuss the existence of the $\tilde{C}$–$\tilde{B}$ transition hereafter.

By combining the thermochemical[18] and spectroscopic data[17,19] with the electronic energy of He(2 ^{3}S), 19.82 eV,

formation processes for the observed species that are energetically possible from $SiCl_4$ and $GeCl_4$ are as follows:

$$He(2\,^3S) + SiCl_4 \rightarrow SiCl(B^2\Sigma^+) + Cl + Cl_2 + He + 5.55\ eV \quad (3a)$$

$$He(2\,^3S) + SiCl_4 \rightarrow SiCl(B^2\Sigma^+) + 3Cl + He + 3.03\ eV, \quad (3b)$$

$$He(2\,^3S) + SiCl_4 \rightarrow SiCl(B'^2\Delta) + Cl + Cl_2 + He + 5.36\ eV, \quad (4a)$$

$$He(2\,^3S) + SiCl_4 \rightarrow SiCl(B'^2\Delta) + 3Cl + He + 2.84\ eV, \quad (4b)$$

$$He(2\,^3S) + SiCl_4 \rightarrow SiCl(C^2\Pi) + Cl + Cl_2 + He + 4.67\ eV, \quad (5a)$$

$$He(2\,^3S) + SiCl_4 \rightarrow SiCl(C^2\Pi) + 3Cl + He + 2.15\ eV, \quad (5b)$$

$$He(2\,^3S) + SiCl_4 \rightarrow SiCl_4^+(\tilde{C}^2T_2) + He + e^- + 4.55\ eV, \quad (6)$$

$$He(2\,^3S) + GeCl_4 \rightarrow Ge(5s^3P_0) + 2Cl_2 + He + 6.13\ eV, \quad (7a)$$

$$He(2\,^3S) + GeCl_4 \rightarrow Ge(5s^3P_0) + 2Cl + Cl_2 + He + 3.61\ eV, \quad (7b)$$

$$He(2\,^3S) + GeCl_4 \rightarrow Ge(5s^3P_0) + 4Cl + He + 1.09\ eV, \quad (7c)$$

$$He(2\,^3S) + GeCl_4 \rightarrow GeCl(A^2\Delta) + Cl + Cl_2 + He + 5.63\ eV, \quad (8a)$$

$$He(2\,^3S) + GeCl_4 \rightarrow GeCl(A^2\Delta) + 3Cl + He + 5.63\ eV, \quad (8b)$$

$$He(2\,^3S) + GeCl_4 \rightarrow GeCl_4^+(\tilde{C}^2T_2) + He + e^- + 4.94\ eV, \quad (9)$$

where Cl atom and Cl_2 are in the ground state.

The $5s^3P_{0,1,2}$ and $5s^1P_1$ states of Ge atom have been observed in this study from $GeCl_4$, while neither the emission from the next $5p^1P$ state nor that from other higher states of Ge I was identified. The formation of the $5p^1P$ state via process 7c is exothermic only 0.02 eV. Thus, the observed result leads to the conclusion that Ge atoms are produced via process 7c and that processes 7a and 7b are negligible. We have no experimental information on the formation process for the other neutral species. Although the weak Cl_2^* emission appeared in the spectrum from $GeCl_4$, we do not discuss its formation. From the thermochemical viewpoint, the $\tilde{D}^2A_1$ state of $SiCl_4^+$ and $GeCl_4^+$ was observed in the photoelectron spectra of both parents,[17] but no emission from this state was identified because of predissociation.[4]

Branching Ratios of Excited Ge I States. Table 1 lists relative intensities for the Ge I lines observed from $GeCl_4$. The Ge I line at 265 nm consists of the $5s^3P_2 \rightarrow 4p^{23}P_2$ and $5s^3P_1 \rightarrow 4p^{23}P_0$ transitions. We failed to resolve this peak in the measurement with the optical resolution of 0.06 nm since the wavelength difference between these transitions is estimated to be 0.04 nm. Thus, in order to evaluate the populations for Ge I states, the intensity of the 265 nm line was distributed to two transitions according to the ratio of the corresponding line strengths estimated in an intermediate coupling case; the intensity ratios among the lines from the $5s^3P_1$ state were found to deviate from those calculated by using theoretical line strengths in both *LS*- and *jj*- coupling limits.[20] Owing to the observed ratios for the $5s^3P_1$ state, the intensity of the $^3P_1 \rightarrow {}^3P_0$ component relative to that of the $^3P_2 \rightarrow {}^3P_2$ component at 265 nm was derived to be 0.35. This indicates that the coupling for Ge I is nearly to the *LS*-coupling. Other bands that may affect the populations of the upper states for the seven observed lines were very weak in the 200—700 nm range.

Table 1. Relative Intensities for Ge I Resonance Lines Produced from $GeCl_4$

Transition	λ/nm	Relative intensity
$5s^3P_2 \rightarrow 4p^2\,^3P_1$	259.2	0.28±0.05
$5s^3P_2 \rightarrow 4p^2\,^3P_2$	265.1	0.74[a]
$5s^3P_1 \rightarrow 4p^2\,^3P_0$	265.1	0.26[a]
$5s^3P_1 \rightarrow 4p^2\,^3P_1$	269.1	0.21±0.02
$5s^3P_0 \rightarrow 4p^2\,^3P_1$	271.0	0.28±0.02
$5s^3P_1 \rightarrow 4p^2\,^3P_2$	275.5	0.39±0.03
$5s^1P_1 \rightarrow 4p^2\,^1D_2$	303.9	0.25±0.02
$5s^3P_1 \rightarrow 4p^2\,^1D_2$	327.0	0.064±0.01

a) The intensity ratio between the $^3P_2 \rightarrow {}^3P_2$ and $^3P_1 \rightarrow {}^3P_0$ transitions was derived from the corresponding line strengths estimated in an intermediate coupling case (see text).

When all emission lines from the upper state i of Ge I are measured, the relative population $N(i)$ for the i state can be evaluated by

$$N(i) \propto R(i) = \sum_j R_{ij}, \quad (10)$$

where R_{ij} is the emission intensity for the $i \rightarrow j$ transition and $R(i)$ represents the total emission intensity for the i state. The radiative lifetimes for the observed Ge I states are very short[21] so that the populations are not affected by the difference in the lifetime. Total emission intensity (R) of the Ge I states evaluated and their relative populations normalized by the degeneracy, $N/(2J+1)$, are listed in Table 2. The populations of Ge I thus obtained can be represented by a Boltzmann temperature of 3200±700 K. On the assumption that this temperature can be applied to the populations of all states of Ge I, the average electronic excitation energy of Ge I was estimated to be 0.28±0.06 eV.

This may be compared with the value estimated from equipartition of the available energy among all degrees of freedom on the assumption that reaction 7 proceeds via an long-lived intermediate between $He(2\,^3S)$ and $GeCl_4$; the available energy of 5.73 eV for reaction 7 is distributed statistically among 19 degrees of freedom, neglecting the electronic energy of four Cl atoms. The available energy divided by the degrees of freedom, 0.30 eV, agrees with the value obtained from population analysis of Ge I states. The similar trend was observed for Sn I produced from the collision of

Table 2. Total Emission Intensities (R) and Relative Populations for the Excited Ge I States Produced from $GeCl_4$

Upper state	E/eV[a]	τ/ns[b]	R	$N/(2J+1)$[c]
$5s^3P_0$	4.643	3.6	0.28±0.02	100
$5s^3P_1$	4.675	3.7	0.82±0.04	109±6
$5s^3P_2$	4.850	4.0	1.12±0.04	72±6
$5s^1P_1$	4.962	4.0	0.25±0.02	30±8

a) The E is the electronic energy of germanium atom. b) The radiative lifetime; Ref. 21. c) Relative population normalized by the degeneracy.

He(2 ^{3}S) with $SnCl_4$.[5]

Emission Cross Sections. In the emission spectra, the intensity in the wavelength region longer than 710 nm for $SiCl_4$ (Fig. 1) and that longer than 760 nm for $GeCl_4$ (Fig. 3) lack reproducibility because of the low sensitivity of the optical detecting system. Therefore, we have estimated the contribution from the longer wavelength side to evaluate σ_{em} for the $\tilde{C}$–$\tilde{A}$ band. In the analysis, the $\tilde{C}$–$\tilde{A}$ band of $SiCl_4^+$ and the $\tilde{C}$–$\tilde{X}$ and $\tilde{C}$–$\tilde{A}$ bands of $GeCl_4^+$ were fitted to single Gaussian functions by a least-squares method. The best-fitted functions are shown in Figs. 1 and 3. The contribution of the longer wavelength side to the total intensity was estimated to be (13±3)% for the $SiCl_4^+(\tilde{C}$–$\tilde{A})$ band and (5±2)% for the $GeCl_4^+(\tilde{C}$–$\tilde{A})$ band. Table 3 lists the σ_{em} values for several transitions obtained at an E_R of 150 meV; the uncertainty attached to the σ_{em} values includes both the uncertainty (9%) in the σ_{em} for the reference reaction and the experimental errors (4—13%). The σ_{em} value summed up about all Ge I lines from $GeCl_4$ was evaluated to be $(11.3\pm0.9)\times10^{-22}$ m^2; the value is 1/9 of that for Sn I produced from the He(2 ^{3}S)+$SnCl_4$ reaction.[5] On the contrary, formation of Si I from $SiCl_4$ was negligible in this experiment and formation of C I was also negligible in the He(2 ^{3}S)+CCl_4 reaction.[22] In the reaction of He(2 ^{3}S) with Group 14 tetrachlorides (MCl_4), it is concluded that formation of neutral M atom increases with heavier homologues. This tendency probably originates in the fact that an increase of the principal quantum number for valence electrons raises the state density of the electronic state for neutral M atom but reduces the dissociation energy of M–Cl bond. Total σ_{em}'s for $SiCl_4$ and $GeCl_4$ obtained in this experiment is 4.5±0.8 and $(2.2\pm0.4)\times10^{-20}$ m^2, respectively. Thus, the main decay process in the collision of He(2 ^{3}S) with $SiCl_4$ and $GeCl_4$ seems to be Penning ionization.

Collision Energy Dependence of σ_{em}. Figure 4 shows log σ_{em} vs. log E_R plots for the SiCl(B′–X) and $SiCl_4^+(\tilde{C}$–$\tilde{X})$ bands from $SiCl_4$, and Fig. 5 shows those for the Ge I line at 265 nm and the $GeCl_4^+(\tilde{C}$–$\tilde{X})$ band from $GeCl_4$. The observed data were fitted with the function of $\log\sigma_{em} = m\log E_R + C$.[7] The slope m is evaluated to be 0.05±0.04 for the SiCl(B′–X) band and −0.06±0.05 for the $SiCl_4^+(\tilde{C}$–$\tilde{X})$ band produced from $SiCl_4$, and −0.19±0.06 for the Ge I line and −0.10±0.06 for the $GeCl_4^+(\tilde{C}$–$\tilde{X})$ band. The relative intensities among the Ge I lines listed in Table 1 were nearly constant in the collision energy of 120–210 meV. Thus, the dependence of the σ_{em} for other Ge I lines on the collision energy (E_R) is expected to be the same as that of the strongest 265 nm line although other lines were too weak to measure the dependence. We will discuss hereafter the qualitative nature of the slopes rather than quantitative comparisons of them since the kinetic energy distribution of He* beam is relatively broad in this experiment, as mentioned in the previous section. The positive slope reflects the repulsive character of the effective potential between He(2 ^{3}S) and the target molecule which can be related to the repulsive nature of the interaction potential surface peculiar to the geometrical situations where the He(2 ^{3}S) atom approaches the Cl atom of the target molecule, while the negative slope originates in the attractive potential.[7,23]

Table 3. The Emission Cross Sections (σ_{em}) for Several Transitions Resulting from the Collisions of He(2 ^{3}S) with $SiCl_4$ and $GeCl_4$ at E_R of 150 meV

Parent	Transition	$\sigma_{em}/10^{-22}$ m^2
$SiCl_4$	$SiCl(B^2\Sigma^+$–$X^2\Pi)$	2.4±0.8
$SiCl_4$	$SiCl(B'^2\Delta$–$X^2\Pi)$	2.6±0.1
$SiCl_4$	$SiCl(A^2\Sigma^+$–$X^2\Pi)$	1.4±0.3
$SiCl_4$	$SiCl_4^+(\tilde{C}^2T_2$–$\tilde{X}^2T_1)$	153±14
$SiCl_4$	$SiCl_4^+(\tilde{C}^2T_2$–$\tilde{A}^2T_2)$	294±74
$GeCl_4$	Ge I	11.3±0.9
$GeCl_4$	$GeCl(A^2\Delta$–$X^2\Pi)$	1.2±0.2
$GeCl_4$	$GeCl_4^+(\tilde{C}^2T_2$–$\tilde{X}^2T_1)$	73±16
$GeCl_4$	$GeCl_4^+(\tilde{C}^2T_2$–$\tilde{A}^2T_2)$	130±37

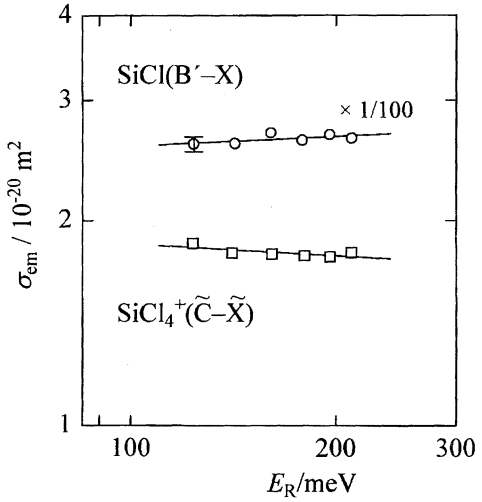

Fig. 4. Collision energy dependences of σ_{em} for the SiCl(B′–X) and $SiCl_4^+(\tilde{C}$–$\tilde{X})$ bands produced from $SiCl_4$.

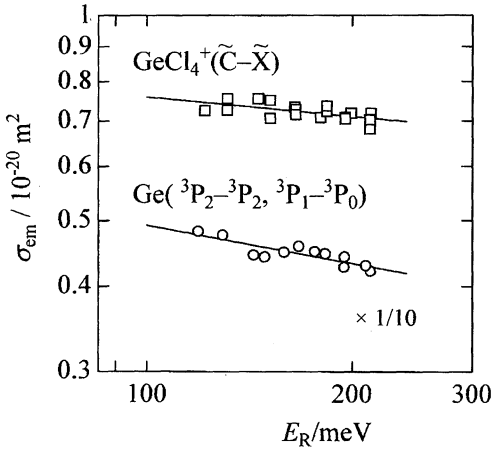

Fig. 5. Collision energy dependences of σ_{em} for the Ge I line and the $GeCl_4^+(\tilde{C}$–$\tilde{X})$ band produced from $GeCl_4$.

Interaction Potentials and Decay Processes. To discuss the observed results concerning the collision energy dependence of σ_{em}'s, the interaction potentials between He(2 ^{3}S) and $SiCl_4$ were calculated using ab initio molecular

orbital (MO) methods. Since there are difficulties associated with calculating the excited states and a well-known resemblance between He($2\,^3$S) and Li($2\,^2$S),[7,24,25] a Li($2\,^2$S) atom was used in place of He($2\,^3$S) in this study. The interaction potentials between a Li($2\,^2$S) atom and $SiCl_4$ were calculated using the Gaussian 94 program package[26] in a UHF scheme and the Møller–Presset perturbation method (MP2) with the frozen core approximation. The standard 6-31+G(d) basis set was used. For all the cases the nuclear positions of $SiCl_4$ were fixed at the geometry optimized before calculating the model potentials. Figure 6 shows the potential-energy curves $V^*(R)$ obtained for $SiCl_4$–He*(Li); R is the distance between the Li atom and Si atom or Cl atom of the target, when the Li atom approaches along several directions. The potential minimums around $R = 0.55$ nm are found to be very shallow (15 meV). We found also the similar minimums (15 meV) around 0.55 nm in the model potentials obtained for $GeCl_4$–He*(Li) in preliminary calculation. Thus, the potential curves for $SiCl_4$ shown in Fig. 6 seem to be applicable to those for $GeCl_4$ as they are.

The collision energy dependences of σ_{em}'s for the $\tilde{C}^2T_2$–$\tilde{X}^2T_1$ band of $SiCl_4^+$ and $GeCl_4^+$ show nearly zero or slightly negative. This is ascribed to the fact that the effective potentials of He($2\,^3$S) with $SiCl_4$ and $GeCl_4$ are nearly zero or slightly attractive. The electron exchange model was succeeded in explanation of the probability for partial Penning ionization observed by Penning ionization electron spectroscopy (PIES) and its collision energy dependence.[7,27]

The electron configuration of the valence shell of MCl_4 (M = Si, Ge) with T_d symmetry is obtained as $...(1a_1)^2(1t_2)^6(2a_1)^2(2t_2)^6(1e)^4(3t_2)^6(1t_1)^6$ except for core orbitals. Three outer orbitals are mostly occupied by nonbonding electrons of Cl atoms (n_{Cl}), while the $2a_1$ and $2t_2$ orbitals have the almost sigma type character of M–Cl (σ_{M-Cl}). Unfortunately, very little is known about PIES of $SiCl_4$ and $GeCl_4$ and the collision energy dependence. Nevertheless,

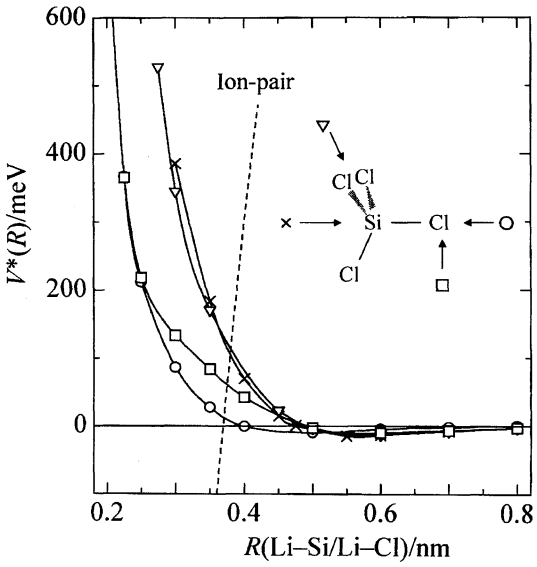

Fig. 6. Model potential curves $V^*(R)$ for $SiCl_4$–He*(Li); R is the distance between Li and Si atom or Cl atom.

when He($2\,^3$S) approaches a Cl atom the interaction between He($2\,^3$S) and the Cl chromophore seems to be similar to that for $C(CH_3)_3Cl$. In a PIES study of He($2\,^3$S) with $C(CH_3)_3Cl$,[27] the $7e(n_{Cl})$ bands shows negative collision energy dependence, but the $11a_1(\sigma_{M-Cl})$ bands shows slightly positive dependence. The $\tilde{C}^2T_2$ state of MCl_4^+ ion corresponds to electron removal from the $2t_2(\sigma_{M-Cl})$ orbital. Therefore, the nearly zero or the slightly negative slope for the $MCl_4^+(\tilde{C}$–$\tilde{X})$ band in this study seems to be inconsistent with the result of the $11a_1$ bands in the PIES of $C(CH_3)_3Cl$. This discrepancy probably originates in the difference in the interaction of He($2\,^3$S) with the Cl_4 chromophore and with the Cl chromophore; for instance, the shapes of the t_2 orbital for CCl_4 are very different from that of the a_1 orbital for CH_3Cl.[28]

On the other hand, the simple electron exchange model proposed for Penning ionization cannot describe neutral fragmentation induced by collision with He($2\,^3$S). Thus, we proposed a model based on the excitation transfer mechanism followed by predissociation in order to describe neutral fragmentation of methyl chlorides.[23] For the He($2\,^3$S) and $SiCl_4$ or $GeCl_4$ system, even if products are branched into ionic states by Penning ionization and neutral fragments by dissociation in exit channels, the entrance potential surface is considered to be the same. This does not necessarily mean that the effective slope obtained for the excited fragment becomes the same as for final ionic state. The slope obtained for the fragment should be considered as a parameter reflecting effective distance where electronic transitions correlating with its formation occur. The slightly positive slope obtained for the SiCl(B′–X) band indicates that the effective distance between He($2\,^3$S) and $SiCl_4$ is rather short, around the classical turning point. The negative slope for the Ge I line indicates that the effective potential of He($2\,^3$S) with $GeCl_4$ is slightly attractive and that the effective distance for the electronic transition is expected to be longer than the classical turning point. The attractive potential originates mainly in the long-range dispersion force. This trend is compatible with the reaction scheme that formation of Ge I from $GeCl_4$ is started via a harpoon mechanism.[29] Thus, a harpoon mechanism and excitation transfer mechanism are candidates for the initial step for formation of Ge I from $GeCl_4$.

When the He($2\,^3$S) atom approaches a certain distance from $GeCl_4$, the electronic state should become modified and mixed with various excitation configurations, which are energetically almost resonant with the initial excitation configuration of He($2\,^3$S). Despite mixing, electronic configurations may be expressed in terms of frozen orbital representations of He($2\,^3$S) and $GeCl_4$. In the first stage of the excitation transfer mechanism, an electron of $GeCl_4$ will transfer to the vacant $1s$ orbital of He($2\,^3$S) and then the $2s$ electron of He($2\,^3$S) has to transfer to some orbitals of $GeCl_4$. Such an energy transfer is considered to be probable when the energy of some orbital for $GeCl_4$ is nearly equal to that of the He $1s$ orbital. Similarly, the orbital energy of an unoccupied orbital of $GeCl_4$ needs to be approximately equal to that of

the He(2 ^{3}S) 2*s* orbital. However, any orbital of $GeCl_4$ is at least 5 eV away from the He 1*s* orbital; the orbital energies of $1t_2$ and $2a_1$ are -30.4 and -20.0 eV, respectively, while the ionization energy of He atom is 24.6 eV. Although we have no information on the virtual orbitals for $GeCl_4$, we prefer the harpoon mechanism from the consideration on the statistical nature of populations for Ge I states as we discuss in the next section.

The first stage of the harpoon mechanism is described as the transfer of a He(2 ^{3}S) 2*s* electron to a vacant outer orbital of $GeCl_4$. The resulting attractive Coulomb force brings a produced ion pair together. The potential surface of the ion pair will be crossed over with several surfaces correlating to formation of excited Ge I at a finite separation. The ion-pair will decay around the crossing point to neutral exit channels via predissociation, and then the ion-pair intermediate is expected to have a longer lifetime. This gives rise to a statistical nature of Ge I state distribution. The intermolecular distance between $GeCl_4$ and He(2 ^{3}S), where the potential surface of He(2 ^{3}S)+$GeCl_4$ crosses with that of He^++$GeCl_4^-$ can be estimated from the following assumptions:

(i) the attractive potential between the He^++$GeCl_4{}^-$ ion pair is approximated by a Coulomb force,

(ii) the repulsive and long-range attractive potentials between He(2 ^{3}S) and $GeCl_4$, $V^*(R)$, are almost equal to those for $SiCl_4$ shown in Fig. 6.

There is very little data about the electron affinity (EA) for group 14 tetrachlorides;[30,31] the only data for $GeCl_4$ is 0.87 eV.[30] Taking into account the ionization potential of He(2 ^{3}S), 4.77 eV, the crossing point is estimated to be 0.37 nm from the estimated ion-pair potential curve (see Fig. 6). Nevertheless, the distance thus obtained seems to be rather short since the effective potentials for formation of Ge I are found to be slightly attractive. It can be concluded that the EA for $GeCl_4$ should be larger than the reported value. We need a more reliable value of EA for further discussion on reaction processes.

We have concluded that the measurement of collision energy dependence of emission cross sections for excited fragments is useful for studying the interaction potential correlating with neutral fragmentation. The knowledge concerning interactions of a 2*s* electron of He with vacant orbitals of target molecules seems to be important for further discussion on dissociation dynamics of Group 14 tetrachlorides.

References

1 M. Tsuji, T. Mizuguchi, and Y. Nishimura, *Can. J. Phys.*, **59**, 985 (1981).

2 M. Tsuji, Y. Nishimura, and T. Mizuguchi, *Chem. Phys. Lett.*, **83**, 483 (1981).

3 M. Tsuji, T. Mizuguchi, and Y. Nishimura, *Chem. Phys. Lett.*, **84**, 318 (1981).

4 I. R. Lambert, S. M. Mason, R. P. Tuckett, and A. Hopkirk, *J. Chem. Phys.*, **89**, 2675 (1988).

5 I. Tokue, Y. Sakai, M. Kobayashi, and K. Yamasaki, *Bull. Chem. Soc. Jpn.*, **69**, 2815 (1996).

6 I. Tokue, T. Kudo, and Y. Ito, *Chem. Phys. Lett.*, **199**, 435 (1992).

7 K. Ohno, T. Takami, K. Mituke, and T. Ishida, *J. Chem. Phys.*, **94**, 2675 (1991).

8 R. A. Sanders, A. N. Schweid, M. Weiss, and E. E. Muschlitz, Jr., *J. Chem. Phys.*, **65**, 2700 (1976).

9 F. J. Comes and F. Speier, *Chem. Phys. Lett.*, **4**, 13 (1969).

10 R. D. Verma, *Can. J. Phys.*, **42**, 2345 (1964).

11 G. A. Oldershaw and K. Robinson, *J. Mol. Spectrosc.*, **38**, 306 (1971).

12 S. R. Singhal and R. D. Verma, *Can. J. Phys.*, **49**, 407 (1971).

13 C. E. Moore, "Atomic Energy Levels II," Natl. Stand. Ref. Data Ser., U.S. Government Printing Office, Washington (1971), p. 136.

14 R. W. B. Pearse and A. G. Gaydon, "The Identification of Molecular Spectra," 4th ed, Chapman and Hall, London (1976).

15 K. B. Rao and P. B. V. Haranath, *J. Phys., B*, **B2**, 1080 (1969).

16 G. A. Oldershaw and K. Robinson, *Trans. Faraday Soc.*, **66**, 532 (1970).

17 P. J. Bassett and D. R. Lloyd, *J. Chem. Soc. A*, **1971**, 641.

18 D. D. Wagman, W. H. Evans, V. B. Parker, R. H. Schumm, I. Halow, S. M. Bailey, K. L Churney, and R. L. Nuttall, *J. Phys. Chem. Ref. Data*, **11**, No. 2 (1982).

19 K. P. Huber and G. Herzberg, "Molecular Spectra and Molecular Structure," "Vol. 4, Constants of Diatomic Molecules," Van Nostrand-Reinhold, New York (1979).

20 E. U. Condon and G. H. Shortley, "The Theory of Atomic Spectra," Cambridge Univ. Press, London (1967).

21 A. A. Radzig and B. M. Smirnov, "Reference Data on Atoms, Molecules, and Ions," Springer-Verlag, Berlin (1985), p. 239.

22 I. Tokue, H. Tanaka, and K. Yamasaki, to be published.

23 I. Tokue, Y. Sakai, and K. Yamasaki, *J. Chem. Phys.*, **106**, 4491 (1997).

24 K. Ohno and S. Sunada, *Proc. Indian Acad. Sci.*, **106**, 327 (1994).

25 H. Yamakado, M. Yamaguchi, S. Hoshino, and K. Ohno, *J. Phys. Chem.*, **99**, 17096 (1995).

26 M. J. Frisch, G. W. Trucks, H. B. Schlegel, P. M. W. Gill, B. G. Johnson, M. A. Robb, J. R. Cheeseman, T. Keith, G. A. Petersson, J. A. Montgomery, K. Raghavachari, M. A. Al-Laham, V. G. Zakrzewski, J. V. Ortiz, J. B. Foresman, C. Y. Peng, P. Y. Ayala, W. Chen, M. W. Wong, J. L. Andres, E. S. Replogle, R. Gomperts, R. L. Martin, D. J. Fox, J. S. Binkley, D. J. Defrees, J. Baker, J. P. Stewart, M. Head-Gordon, C. Gonzalez, and J. A. Pople, "Gaussian 94, Revision B.2," Gaussian, Inc., Pittsburgh, PA (1995).

27 T. Takami, K. Mitsuke, and K. Ohno, *J. Chem. Phys.*, **95**, 918 (1991).

28 K. Kimura, S. Katsumata, Y. Achiba, T. Yamazaki, and S. Iwata, "Handbook of HeI Photoelectron Spectra of Fundamental Organic Molecules," Japan Sci. Soc. Press, Tokyo (1981).

29 R. D. Levine and R. B. Bernstein, "Molecular Reaction Dynamics and Chemical Reactivity," Oxford Univ. Press, Oxford (1987).

30 M. Hatano and O. Ito, *Bull. Chem. Soc. Jpn.*, **44**, 916 (1971).

31 K. Lacman, M. J. P. Maneira, A. M. C. Moutinho, and U. Weigmann, *J. Chem. Phys.*, **78**, 1767 (1983).